

Final Technical Report

Award Number: DE-SC0016359

University: University of Kansas Center for Research, Inc.

Project Title: Mechanistic Studies to Enable Aerobic Oxidation of C-H Bonds by Manganese Catalysts

Principal Investigator: Timothy A. Jackson

Executive Summary

The project Mechanistic Studies to Enable Aerobic Oxidation of C-H Bonds by Manganese Catalysts provided fundamental new insight into the factors affecting hydrocarbon oxidation reactions by manganese-oxo complexes. These insights stem from the development of a structure-function relationship, whereby particular molecular properties of manganese(IV)-oxo complexes were shown to correlate to their efficacy in hydrocarbon oxidation reactions. This work is important, as manganese oxidation catalysts have seen increasing use in synthetic transformations, including reactions relevant to the synthesis of pharmaceuticals and other value-added chemicals. The desirability of developing new manganese catalysts stems from the inexpensive nature and low toxicity of the metal manganese, which contrasts with the high cost and toxicity of many other metals. The work carried out by this project was disseminated to the scientific community in the form of 14 peer-reviewed publications and over twenty presentations. In addition, the research results were incorporated into graduate and undergraduate courses at the University of Kansas, providing additional means of dissemination.

Comparison of Actual Accomplishments and Objectives

The objectives of this project are as follows: (1) identify relationships between ligand properties and O₂ activation by Mn^{II} centers; (2) evaluate the two-state reactivity model of Mn^{IV}-oxo adducts using a combination of experiment and theory; and (3) understand variations in ligand-field effects on the reactivity of Mn^{IV}-oxo and Fe^{IV}-oxo complexes. The outcomes of this project directly addressed these objectives. Research supported by the project uncovered different O₂ activation pathways for a pair of Mn^{II} complexes and demonstrated that these different pathways were caused by the steric properties of the supporting ligand (publication #7). A series of experimental and computational studies provided a detailed assessment of the two-state reactivity model for Mn^{IV}-oxo complexes and demonstrated how predictions made by this model could be used to design some of the most active Mn^{IV}-oxo complexes known to date (publications #1, 2, 4, 5, 8, 9 12, and 13 below). Finally, investigations of Mn^{IV}-oxo complexes revealed different reactivity trends when compared to their Fe^{IV}-oxo analogues (publication #6 and 10 below).

Summary of Project Activities

The majority of the project outcomes have been reported in the 14 peer-reviewed publications. These activities are summarized below.

O_2 Activation by Mn^{II} Centers. Previous work with synthetic Mn^{II} complexes capable of O_2 activation has offered two primary reactive mechanisms. In most cases, Mn^{II} complexes are oxidized to form high-valent Mn^{IV} -oxo species that undergo comproportionation reactions with residual Mn^{II} in solution and form oxo-bridged $Mn^{III}Mn^{III}$ dimers (Coggin, M. K. *et al.*, *Inorg. Chem.* **2012**, *51*, 6633). In contrast, for Mn^{II} species with sterically-encumbered reactive sites, the Mn^{IV} -oxo intermediate is proposed to carry out H-atom transfer from solvent molecules to form monomeric Mn^{III} -hydroxo species instead (Shirin, Z. *et al.*, *Chem. Commun.* **1997**, 1967). Our efforts towards understanding dioxygen activation have focused on the Mn^{II} complexes $[Mn^{II}(dpaq)(OTf)]$ and the sterically modified $[Mn^{II}(dpaq^{2Me})(OTf)]$ (Figure 1). We had previously shown that each of these complexes reacts with O_2 to form mononuclear Mn^{III} -hydroxo species in >96% isolated yields. In this last funding period, we performed O_2 titration experiments with $[Mn^{II}(dpaq)(OTf)]$, which showed a 4:1 Mn^{II} : O_2 stoichiometry (Figure 2).

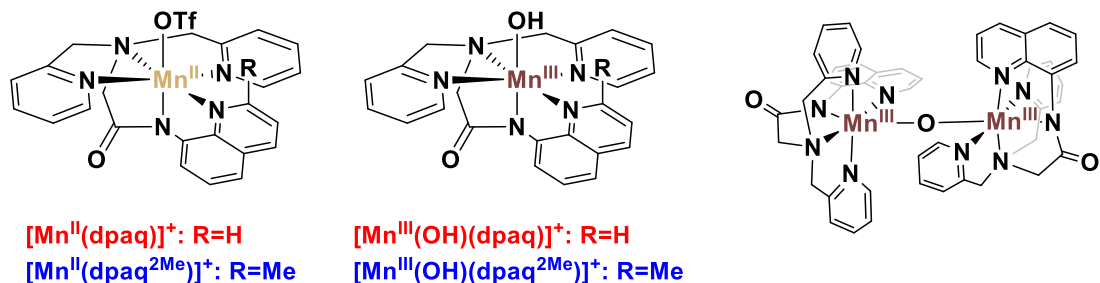


Figure 1. Molecular structures of Mn^{II} complexes, $[Mn^{II}(dpaq)(OTf)]$ and $[Mn^{II}(dpaq^{2Me})(OTf)]$ (left); Mn^{III} -hydroxo complexes, $[Mn^{III}(OH)(dpaq)]^+$ and $[Mn^{III}(OH)(dpaq^{2Me})]^{+}$ (center); and oxo-bridged $Mn^{III}Mn^{III}$ dimer, $[Mn^{III}Mn^{III}(\mu-O)(dpaq)_2]^+$ (right).

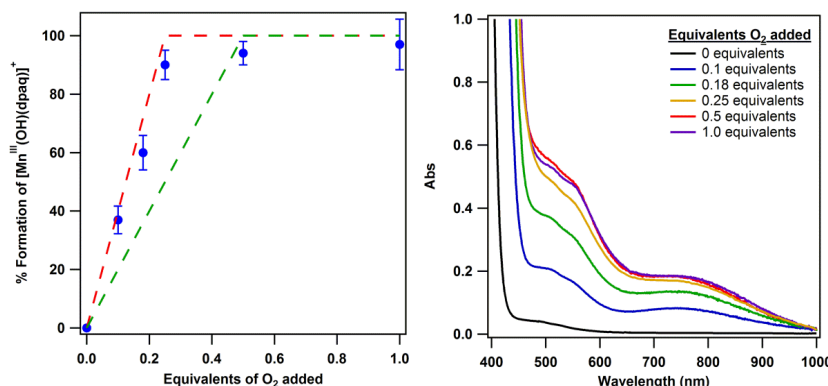


Figure 2. Left: Plot of O_2 titration data (blue) showing percent formation of **1a** as a function of added O_2 . Trend lines for 4:1 (red) and 2:1 (green) Mn : O_2 stoichiometry are shown for comparison. Right: Electronic absorption spectra for MeCN solutions of **1** treated with varying equivalents of O_2 at $20^\circ C$.

We have also been able to trap and characterize an oxo-bridged $Mn^{III}Mn^{III}$ intermediate that converts to the Mn^{III} -hydroxo product through hydrolysis with adventitious H_2O . Collectively, these data support an O_2 activation mechanism where a transient Mn^{IV} -oxo intermediate is trapped by unreacted Mn^{II} to form the oxo-bridged $Mn^{III}Mn^{III}$ species (Figure 3).

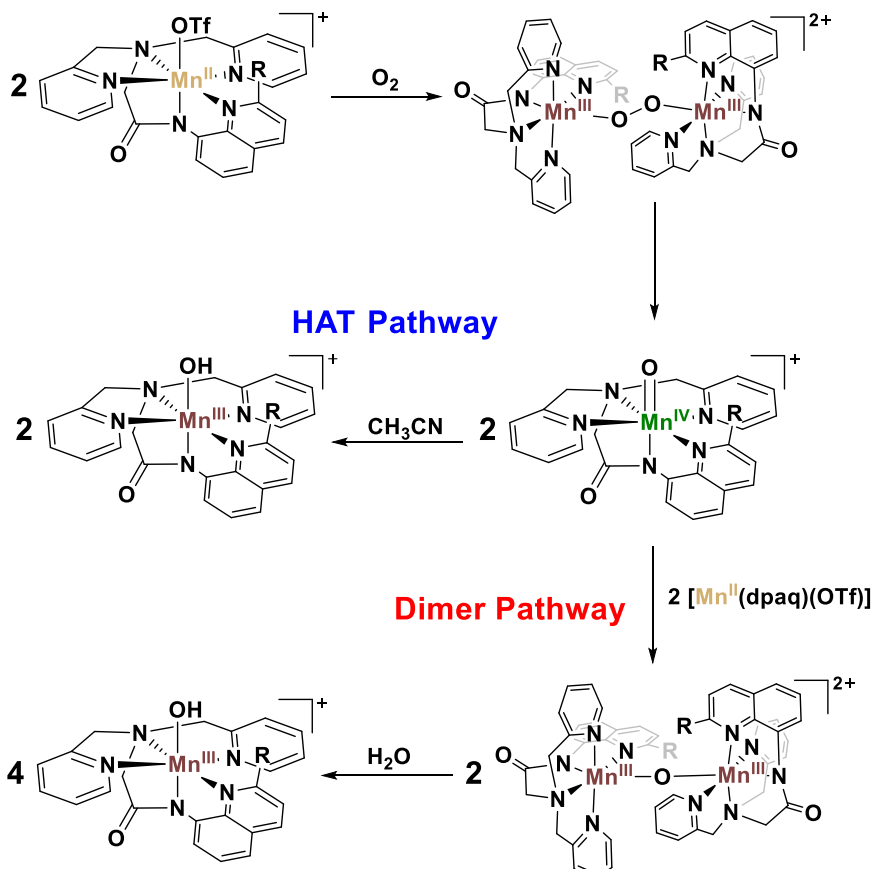


Figure 3. Proposed pathways for dioxygen activation and subsequent Mn^{III}-hydroxide formation by $[\text{Mn}^{\text{II}}(\text{dpaq})]^+$ and $[\text{Mn}^{\text{II}}(\text{dpaq}^{2\text{Me}})]^+$. For $[\text{Mn}^{\text{II}}(\text{dpaq})(\text{OTf})]$, a Mn^{IV}-oxo intermediate is trapped by residual $[\text{Mn}^{\text{II}}(\text{dpaq})(\text{OTf})]$ in solution to form an oxo-bridged Mn^{III}Mn^{III} dimer that undergoes hydrolysis to give the observed Mn^{III}-hydroxide product (dimer pathway). In the case of the sterically modified $[\text{Mn}^{\text{II}}(\text{dpaq}^{2\text{Me}})(\text{OTf})]$ complex, dimerization between the proposed Mn^{IV}-oxo species and residual Mn^{II} complex in solution is hindered. Instead, the Mn^{IV}-oxo species abstracts a H atom from solvent to form a monomeric Mn^{III}-hydroxide species (HAT pathway).

Investigations of the sterically modified $[\text{Mn}^{\text{II}}(\text{dpaq}^{2\text{Me}})(\text{OTf})]$ complex provided strong evidence for an alternate pathway to the Mn^{III}-hydroxido product. The sterically modified complex reacts with dioxygen at a much slower rate than $[\text{Mn}^{\text{II}}(\text{dpaq})(\text{OTf})]$, and investigations to date have provided no evidence for the formation of an oxo-bridged Mn^{III}Mn^{III} species. Instead, only the monomeric Mn^{III}-hydroxido species is observed from reaction with O₂. Reactions between $[\text{Mn}^{\text{II}}(\text{dpaq}^{2\text{Me}})]^+$ and O₂ in deuterated acetonitrile result in the formation of the Mn^{III}-OD product, supporting a mechanism in which the transient Mn^{IV}-oxo species abstracts a H (or D) atom from solvent, as opposed to being sequestered by unreacted Mn^{II} in solution (Figure 3). Presumably, the steric bulk of the methyl-quinolinyl group hinders the formation of the oxo-bridged Mn^{III}Mn^{III} dimer, showing the effect of even slight ligand modifications on dioxygen activation. These studies are described in more detailed in publication #7.

C-H Bond Activation by Mn^{IV}-oxo Complexes. In recent years, the reactivity of mononuclear Mn^{IV}=O complexes has been proposed to operate by a two-state model (see Cho,

K.-B.; Shaik, S.; Nam, W., "Theoretical Investigations into C–H Bond Activation Reaction by Nonheme Mn^{IV}O Complexes: Multistate Reactivity with No Oxygen Rebound." *The Journal of Physical Chemistry Letters* **2012**, 3 (19), 2851–2856.). According to this model, a ⁴E excited state offers a lower-energy transition state for hydrogen-atom transfer than the ⁴B₁ ground state. Although this model has been used to rationalize the reactivity of several Mn^{IV}-oxo adducts for both hydrogen-atom and oxygen-atom transfer reactions, it is lacking experimental support. To test this model, we first used a combination of electronic absorption and magnetic circular dichroism (MCD) spectroscopies to determine the energy of the ⁴E excited state for our previously reported [Mn^{IV}(O)(N4py)]²⁺ complex. Because this state arises from a one-electron transition from quasi-degenerate Mn^{IV} 3d_{xz}/3d_{yz} MOs to the Mn^{IV} 3d_{x²-y²} MO, it is expected to give rise to a pseudo-A term in the MCD spectrum (a derivative-shaped feature with increased intensity at lower temperature). On the basis of these selection rules, we were able to assign a near-IR electronic transition of [Mn^{IV}(O)(N4py)]²⁺ as the ⁴E excited state. Importantly, the experimental energy of this state is significantly higher than that predicted by DFT computations. Using wavefunction-based CASSCF/NEVPT2 calculations, we showed that the energetic splitting of the ⁴B₁ and ⁴E states remains fairly constant as the Mn-oxo bond is elongated (*i.e.*, along the hydrogen-atom transfer reaction coordinate in the absence of substrate). However, these calculations also revealed that the ⁴E state develops significant Mn^{III}-oxyl character upon even modest Mn-O bond elongation. Insofar as radical character is important for hydrogen-atom transfer reactions, these results reinforce the previous prediction that the ⁴E state should be more reactive for C-H bond oxidation than the ⁴B₁ ground state. Thus, if the ⁴E state were to be stabilized through interactions with substrate, this state could provide a potent reaction channel for substrate oxidation. These accomplishments are described in publication #1.

Of the current Mn^{IV}-oxo complexes known to effect C-H bond oxidation processes, large variations in supporting ligands and reaction conditions prevent a fundamental understanding of the factors that govern reactivity. To address this challenge, we employed a series of derivatives of the N4py ligand to generate two new Mn^{IV}-oxo complexes with systematically perturbed properties. In particular, we employed electron-rich and electron-deficient ligand derivatives to determine the influence of equatorial ligand donor strength on Mn^{IV}-oxo properties. One of the new complexes, [Mn^{IV}(O)(2pyN2Q)]²⁺ (see Figure 4), which contains weaker equatorial interactions, showed significant rate enhancements in C-H bond oxidation and sulfur-oxidation reactions compared to [Mn^{IV}(O)(N4py)]²⁺. On the other hand, the [Mn^{IV}(O)(^{DMM}N4py)]²⁺ complex, which contains stronger Mn-N equatorial interactions, showed significant decreases in oxidation reaction rates compared to [Mn^{IV}(O)(N4py)]²⁺. Thus, these studies showed how subtle variations in equatorial donor strength can have a profound effect on reaction rates. The observed rate variations correlate with the energy of the ⁴E excited state, consistent with a computational prediction that this state is important in Mn^{IV}-oxo reactivity. However, our observed reaction rate variations can also be explained in terms of the Mn^{III/IV} reduction potentials, which we measured for our Mn^{IV}-oxo complexes. Thus, the exact rationale for the large rate variations observed for this set of complexes is not certain at present. These accomplishments are described in publication #2.

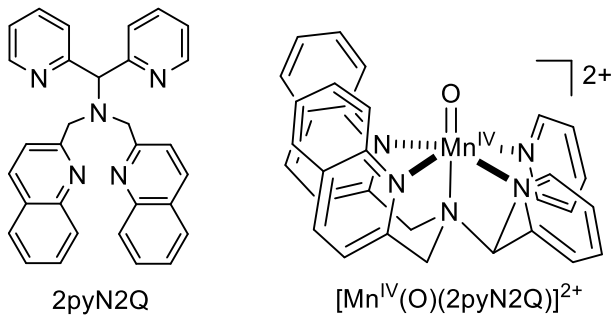
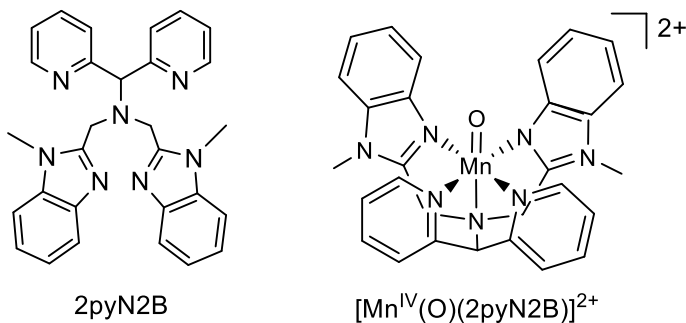


Figure 4. Molecular structures of 2pyN2Q ligand (left) and $[\text{Mn}^{\text{IV}}(\text{O})(\text{2pyN2Q})]^{2+}$ complex (right).

To expand understanding of the influence of the ligand field on reactivity, we developed a new Mn^{IV}-oxo complex supported by an *N*-(methyl)benzimidazolyl analogue (2pyN2B; see Figure 5). We chose this benzimidazolyl derivative, as previous work with Fe^{IV}-oxo systems had shown a 100-fold rate enhancement for C-H bond oxidation for a benzimidazole-containing complex compared to the pyridine-containing analogue. We generated the $[\text{Mn}^{\text{IV}}(\text{O})(\text{2pyN2B})]^{2+}$ complex by idosobenzene oxidation of the Mn^{II} starting material and characterized the Mn^{IV}-oxo complex by a suite of spectroscopic techniques (electronic absorption, electron paramagnetic resonance, and Mn K-edge X-ray absorption spectroscopy, XAS). We also performed XAS studies for other previously reported Mn^{IV}-oxo complexes. Analysis of EXAFS data for these complexes showed Mn=O distances near 1.70 Å. Although these bond lengths are similar to those reported for Mn^{IV}=O adducts, they are ca. 0.02 Å longer than that predicted by density functional theory (DFT) computations. Excellent agreement between the EXAFS and DFT distances was obtained when we considered explicit solvent molecules (2,2,2-trifluoroethanol, TFE) hydrogen-bonding with the oxo ligands (Figure 6). This result suggests that the TFE solvent might play a role in stabilizing Mn^{IV}-oxo species through hydrogen-bonding interactions (we note that a number of Mn^{IV}-oxo adducts can be stabilized in TFE but not in other solvents). Having characterized $[\text{Mn}^{\text{IV}}(\text{O})(\text{2pyN2B})]^{2+}$, we then explored its reactivity in hydrogen- and oxygen-atom transfer reactions, using 9,10-dihydroanthracene and thioanisole as representative substrates. Unexpectedly, the $[\text{Mn}^{\text{IV}}(\text{O})(\text{2pyN2B})]^{2+}$ showed HAT and OAT rates on the *lower* end of those observed for our previously reported Mn^{IV}-oxo complexes. These results demonstrate that ligand design principles identified for Fe^{IV}-oxo complexes cannot be applied carte blanche to Mn^{IV}-oxo species. These results are described in more detail in publications #6 and 9.



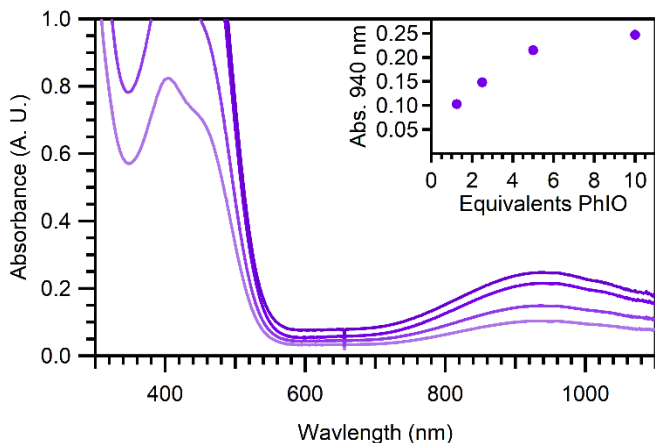


Figure 5. Top: Molecular structures of 2pyN2B ligand (left) and $[\text{Mn}^{\text{IV}}(\text{O})(2\text{pyN2B})]^{2+}$ complex (right). Bottom: Electronic absorption spectrum showing the formation of the $[\text{Mn}^{\text{IV}}(\text{O})(2\text{pyN2B})]^{2+}$ complex by PhIO oxidation of the $[\text{Mn}^{\text{II}}(\text{OH}_2)(2\text{pyN2B})]^{2+}$ precursor. The inset shows the growth of intensity of the near-infrared electronic absorption band of $[\text{Mn}^{\text{IV}}(\text{O})(2\text{pyN2B})]^{2+}$ as a function of equivalents of PhIO.

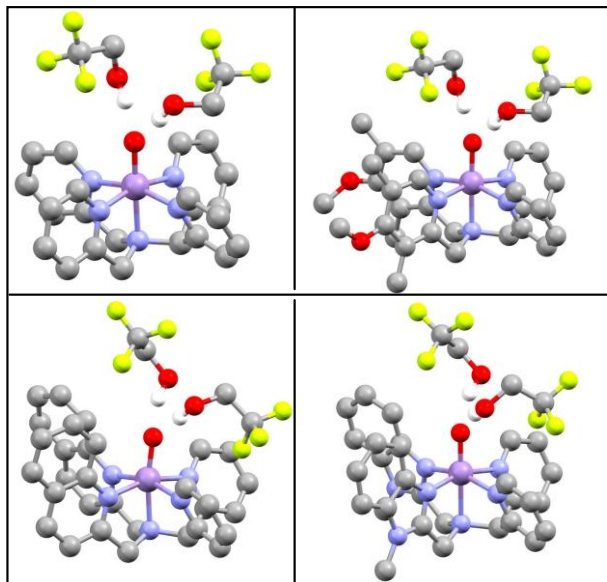


Figure 6. Molecular structures of Mn^{IV} -oxo complexes, $[\text{Mn}^{\text{IV}}(\text{O})(\text{N}4\text{py})]^{2+} \cdot (\text{TFE})_2$ (top-left), $[\text{Mn}^{\text{IV}}(\text{O})(^{\text{DMM}}\text{N}4\text{py})]^{2+} \cdot (\text{TFE})_2$ (top-right), $[\text{Mn}^{\text{IV}}(\text{O})(2\text{pyN2Q})]^{2+} \cdot (\text{TFE})_2$ (bottom-left), and $[\text{Mn}^{\text{IV}}(\text{O})(2\text{pyN2B})]^{2+} \cdot (\text{TFE})_2$ (bottom-right).

To better understand the experimental rates for C-H bond oxidation by Mn^{IV} -oxo species, we explored these reactions using electronic structure methods. Original DFT computations invoked a multi-state reactivity model, involving crossing from the $^4\text{B}_1$ ground state to a low-lying ^4E state, but this prediction lacked experimental validation (Chen, J. *et al.*; *Chem. Comm.* **2015**, 13094). Our initial work in this area (Leto, *et al.*; *J. Am. Chem. Soc.* **2016**, 15413) showed that these Mn^{IV} -oxo complexes contain significant multireference character in both the $^4\text{B}_1$ state and the ^4E states, which calls into question the appropriateness of the DFT method. To explore this issue, we used experimental activation parameters for ethylbenzene oxidation by a Mn^{IV} -oxo complex to compare

DFT (at the B3LYP level) and multi-reference CASSCF-NEVPT2 computations, the latter of which can properly treat multi-reference systems. Both the DFT and CASSCF-NEVPT2 methods predict the ^4E transition state to be at lower energy (Figure 7), with the CASSCF-NEVPT2 result being in reasonable agreement with the experimentally determined energy barrier. In contrast, the DFT results severely underestimate the activation barrier on the ^4E surface, predicting a far faster reaction than observed experimentally. These results demonstrate that a multireference treatment is required to treat Mn^{IV} -oxo systems. This work is described in more detail in publication #8.

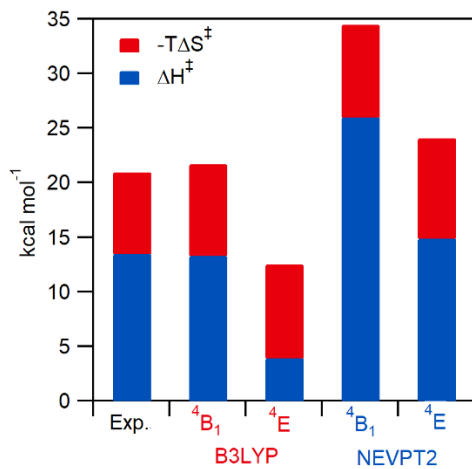


Figure 7. Graph showing the deconvoluted activation barriers into their entropy (at 25 °C) and enthalpy components.

Given the impressive reactivity of several of the Mn^{IV} -oxo complexes, we are expanding our exploration of reactivity to include olefins. These substrates present a challenge of regioselectivity, as the Mn^{IV} -oxo unit can transfer an oxygen atom to the olefin to give an epoxide product, or the Mn^{IV} -oxo unit can abstract an allylic C-H bond to yield an allylic oxidation product. We showed that a set of Mn^{IV} -oxo complexes yielded different olefin epoxidation / allylic oxidation ratios, which could be correlated to changes in the $\text{Mn}=\text{O}$ bond dissociation free energy. This work is described in more detail in publication #13.

As a further means of assessing the best descriptors of reactivity for C-H bond oxidation by Mn^{IV} -oxo complexes, we generated a series of manganese(II) and oxomanganese(IV) complexes supported by neutral, pentadentate ligands with varied equatorial ligand-field strength (N3pyQ, N2py2I, and N4py^{Me2}). These complexes were characterized using structural and spectroscopic methods. On the basis of electronic absorption spectroscopy, the $[\text{Mn}^{\text{IV}}(\text{O})(\text{N4py}^{\text{Me2}})]^{2+}$ complex has the weakest equatorial ligand field among a set of similar Mn^{IV} -oxo species. In contrast, $[\text{Mn}^{\text{IV}}(\text{O})(\text{N2py2I})]^{2+}$ shows the strongest equatorial ligand-field strength for this same series. We examined the influence of these changes in electronic structure on the reactivity of the oxomanganese(IV) complexes using hydrocarbons and thioanisole as substrates. The $[\text{Mn}^{\text{IV}}(\text{O})(\text{N3pyQ})]^{2+}$ complex, which contains one quinoline and three pyridine donors in the equatorial plane, ranks among the fastest Mn^{IV} -oxo complexes in C-H bond and thioanisole oxidation. While a weak equatorial ligand field has been associated with high reactivity, the $[\text{Mn}^{\text{IV}}(\text{O})(\text{N4py}^{\text{Me2}})]^{2+}$ complex is only a modest oxidant. Buried volume plots suggest that steric

factors dampen the reactivity of this complex. Trends in reactivity were examined using DFT-computed bond dissociation free energies (BDFEs) of the Mn^{III}O–H and Mn^{IV}=O bonds. We observe an excellent correlation between Mn^{IV}=O BDFEs and rates of thioanisole oxidation rates, but more scatter is observed between hydrocarbon oxidation rates and the Mn^{III}O–H BDFEs. A manuscript describing this work has been submitted and is presently under review.

Publications

- 1) Leto, D. F.; Massie, A. A.; Rice, D. B.; Jackson, T. A., “Spectroscopic and computational investigations of a mononuclear manganese(IV)-oxo complex reveal electronic structure contributions to reactivity.” *J. Am. Chem. Soc.* **2016**, *138* (47), 15413-15424. <http://dx.doi.org/10.1021/acs.inorgchem.5b02309>
- 2) Massie, A. A.; Denler, M. C.; Cardoso, L. T.; Walker, A. N.; Hossain, M. K.; Day, V. W.; Nordlander, E.; Jackson, T. A., “Equatorial Ligand Perturbations Influence the Reactivity of Manganese(IV)-Oxo Complexes.” *Angew. Chem. Int. Ed.* **2017**, *56* (15), 4178-4182. <http://dx.doi.org/10.1002/anie.201612309>
- 3) Jensen, S. C.; Davis, K. M.; Sullivan, B. T.; Hartzler, D. A.; Seidler, G. T.; Casa, D. M.; Kasman, E.; Colmer, H. E.; Massie, A. A.; Jackson, T. A.; Pushkar, Y. N., “X-ray Emission Spectroscopy of Biomimetic Mn Coordination Complexes.” *J. Phys. Chem. Lett.* **2017**, *8* (11), 2584-2589. <http://dx.doi.org/10.1021/acs.jpclett.7b01209>
- 4) Rice, D. B.; Massie, A. A.; Jackson, T. A., “Manganese–Oxygen Intermediates in O–O Bond Activation and Hydrogen-Atom Transfer Reactions.” *Acc. Chem. Res.* **2017**, *50* (11), 2706-2717. <http://dx.doi.org/10.1021/acs.accounts.7b00343>
- 5) Massie, A. A.; Sinha, A.; Parham, J. D.; Nordlander, E.; Jackson, T. A. “Relationship between Hydrogen-Atom Transfer Driving Force and Reaction Rates for an Oxomanganese(IV) Adduct.” *Inorg. Chem.* **2018**, *57*, 8253-8263. <https://doi.org/10.1021/acs.inorgchem.8b00852>
- 6) Denler, M.C.; Massie, A.A.; Singh, R.; Stewart-Jones, E.; Sinha, A.; Day, V.W.; Nordlander, E.; Jackson, T.A. “Mn^{IV}-Oxo complex of a bis (benzimidazolyl)-containing N5 ligand reveals different reactivity trends for Mn^{IV}-oxo than Fe^{IV}-oxo species,” *Dalton Trans.* **2019**, *48* (15), 5007-5021. <http://dx.doi.org/10.1039/C9DT00308H>
- 7) Parham, J.D.; Wijeratne, G.B.; Mayfield, J.R.; Jackson, T.A. “Steric control of dioxygen activation pathways for Mn^{II} complexes supported by pentadentate, amide-containing ligands,” *Dalton Trans.* **2019**, *48* (34), 13034-13045. <http://dx.doi.org/10.1039/C9DT02682G>
- 8) Rice, D.B.; Massie, A.A.; Jackson, T.A. “Experimental and Multireference ab Initio Investigations of Hydrogen-Atom-Transfer Reactivity of a Mononuclear Mn^{IV}-oxo Complex,” *Inorg. Chem.* **2019**, *58* (20), 13902-13916. <https://doi.org/10.1021/acs.inorgchem.9b01761>

9) Massie, A.A.; Denler, M.C.; Singh, R.; Sinha, A.; Nordlander, E.; Jackson, T.A. “Structural Characterization of a Series of N5-Ligated Mn^{IV}-Oxo Species,” *Chem. Eur. J.* **2020**, *26* (4), 900-912. <https://onlinelibrary.wiley.com/doi/abs/10.1002/chem.201904434>

10) Mayfield, J. R.; Grottemeyer, E. N.; Jackson, T. A. “Concerted proton–electron transfer reactions of manganese–hydroxo and manganese–oxo complexes.” *Chem. Commun.* **2020**, *56*, 9238-9255. <http://dx.doi.org/10.1039/D0CC01201G>

11) Kwon, Y. M.; Lee, Y.; Evenson, G. E.; Jackson, T. A.; Wang, D. “Crystal Structure and C–H Bond-Cleaving Reactivity of a Mononuclear Co^{IV}–Dinitrate Complex.” *J. Am. Chem. Soc.* **2020**, *142*, 13435-13441. <https://doi.org/10.1021/jacs.0c04368>

12) Singh, P.; Stewart-Jones, E.; Denler, M. C.; Jackson, T. A. “Mechanistic insight into oxygen atom transfer reactions by mononuclear manganese(IV)–oxo adducts.” *Dalton Trans.* **2021**, *50*, 3577-3585. <http://dx.doi.org/10.1039/D0DT04436A>

13) Singh, P.; Denler, M. C.; Mayfield, J. R.; Jackson, T. A. “Differences in chemoselectivity in olefin oxidation by a series of non-porphyrin manganese(IV)-oxo complexes.” *Dalton Trans.* **2022**, *51*, 5938-5949. <http://dx.doi.org/10.1039/D2DT00876A>

14) Kwon, Y. M.; Lee, Y.; Schmautz, A. K.; Jackson, T. A.; Wang, D. “C–H Bond Activation by a Mononuclear Nickel(IV)-Nitrate Complex.” *J. Am. Chem. Soc.* **2022**, *144*, 12072-12080. <https://doi.org/10.1021/jacs.2c02454>